Dipolar particles in an external field: Molecular dynamics simulation and mean field theory

Ran Jia and Reinhard Hentschke*
Fachbereich Mathematik und Naturwissenschaften, Bergische Universität, D-42097 Wuppertal, Germany
(Received 30 July 2009; published 5 November 2009)

Using molecular dynamics computer simulation we compute gas-liquid phase coexistence curves for the Stockmayer fluid in an external electric field. We observe a field-induced shift of the critical temperature ΔT_c. The sign of ΔT_c depends on whether the potential or the surface charge density is held constant assuming that the dielectric material fills the space between capacitor plates. Our own as well as previous literature data for ΔT_c are compared to and interpreted in terms of a simple mean field theory. Despite considerable errors in the simulation results, we find consistency between the simulation results obtained by different groups including our own and the mean field description. The latter ties the sign of ΔT_c to the outside constraints via the electric field dependence of the orientation part of the mean field free energy.

DOI: 10.1103/PhysRevE.80.051502 PACS number(s): 64.70.F−, 68.35.Rh, 87.10.Tf, 64.75.Gh

I. INTRODUCTION

Over many years the phase behavior of dipolar liquids has created significant interest (see, in particular, the following reviews [1–4]). Aside from the practical importance many apparently simple model systems have been studied both theoretically and via computer simulation because of the rich and difficult phase behavior due to the addition of dipole-dipole interaction to simple short-ranged fluid potentials. Interesting questions are, for instance, the discrepancy between the "easy" prediction and computer observation of the isotropic-to-ferroelectric transition in models of dipolar fluids and their elusiveness in real low molecular weight liquids possessing rather large molecular dipole moments (e.g., [5,6]). Another question is whether dipole-dipole interaction alone, i.e., without another contribution to particle-particle attraction, can lead to vapor-liquid coexistence (e.g., [7]).

Here we focus on the gas-liquid (g-l) critical point shift, i.e., ΔT_c, in a model dipolar liquid caused by an external electric field. The number of simulation studies computing the field-dependent shift of the g-l critical parameters for dipolar fluids is relatively small [8–11] (see also [12]) even though the much larger number of theoretical works addressing this phenomenon attests to its general and sustained interest (selected examples are [13–22]). In particular the authors of the last of these references, i.e., Ref. [22], emphasize an apparent inconsistency regarding the sign of ΔT_c in the literature discussing the g-l critical temperature shift under the influence of an electric field.

In this work we present simulation results for the critical point shift in a Stockmayer fluid in response to an external electric field if the reduced dipole moment is small. We also look in detail at the available results obtained by other groups via computer simulation and compare them to a simple mean field model based on Onsager's description of liquid dielectrics, which, in our opinion, resolves the inconsistency mentioned above.

*Author to whom correspondence should be addressed; http://constanze.materials.uni-wuppertal.de; hentschk@uni-wuppertal.de

The paper is structured as follows. Section II discusses the molecular dynamics (MD) method. Important details can be found in the Appendix. Section III presents a simple mean field theory useful for the conceptual understanding. The results are compiled in Sec. IV. Section V is the conclusion.

II. SIMULATION METHOD

We carry out MD computer simulations of the Stockmayer fluid in an external electric field. The total potential energy of the system is

$$U = U_{LJ} - \frac{1}{2}\vec{m}_i \mathbf{T}_{ij}\vec{m}_j + \frac{1}{2}\frac{\vec{p}_i^2}{\alpha} - \vec{m}_i \cdot \vec{E}_i^{ext} - \frac{1}{2}g\vec{m}_i \cdot \vec{M}_i \quad (1)$$

(making use of the summation convention). Here U_{LJ} is the sum over all Lennard-Jones (LJ) pair potentials,

$$U_{LJ} = \frac{1}{2}\sum_{i,j=1(i\neq j, r_{ij}<r_{cut})}^{N} 4(r_{ij}^{-12} - r_{ij}^{-6}) + U_{LJ,lrc}, \quad (2)$$

between Stockmayer particles i and j separated by the distance r_{ij}. Notice that for the LJ parameters we assume $\varepsilon = \sigma = 1$. Only particles within the cutoff distance r_{cut} interact explicitly. Interactions from beyond r_{cut} in the case of U_{LJ} are included via the usual long-range correction, $U_{LJ,lrc} = -(8\pi/3)N\rho r_{cut}^{-3}$, where ρ is the particle number density. The remaining terms in Eq. (1) are due to the interaction between point dipole moments,

$$\vec{m}_i = \vec{\mu}_i + \vec{p}_i, \quad (3)$$

located on every LJ site i. The dipole moments are in units of $\sqrt{4\pi\epsilon_o\varepsilon\sigma^3}$ (ϵ_o: vacuum permittivity). Here $\vec{\mu}_i$ is a permanent point dipole moment and $\vec{p}_i$ is an induced point dipole moment computed via

$$\vec{p}_i = \alpha\vec{E}_i, \quad (4)$$

where α is a point polarizability associated with every LJ site. Even though our present results are almost exclusively for $\alpha = 0$, we include the case $\alpha \neq 0$ for sake of latter reference. $\vec{E}_i$ is the total electric field experienced by the particle located at site i given by

$$\vec{E}_i = \mathbf{T}_{ij}\vec{m}_j + \vec{E}_i^{ext} + g\vec{M}_i. \tag{5}$$

The quantity $\mathbf{T}_{ij}$ is the dipole tensor whose Cartesian components $(\alpha,\beta=1,2,3)$ are

$$T_{ij}^{\alpha\beta} = 3\frac{r_{ij}^{\alpha}r_{ij}^{\beta}}{r_{ij}^{5}} - \delta_{\alpha\beta}\frac{1}{r_{ij}^{3}} \tag{6}$$

$(i \neq j)$. $\vec{E}_i^{ext}$ is the external field as it is felt at site i. The external field is assumed constant throughout the volume V of the system. However, we keep the index i as a reminder that the relation between a true external field $\vec{E}^{ext}$, e.g., generated by capacitor plates between which the system is placed, and $\vec{E}_i^{ext}$ does depend on how long-range interactions are handled in the simulation.

Notice that two scenarios are particularly relevant: (i) fixed charge density on the capacitor plates; (ii) fixed potential. Case (i) corresponds to $\vec{E}^{ext}$ held constant. Here $\vec{E}^{ext}$ is the electric field in a slit separating the dielectric from a capacitor plate. Case (ii) corresponds to $\vec{E}^{(\infty)}$ held constant. Here $\vec{E}^{(\infty)}$ is the average or Maxwell field inside the dielectric.

As before for the LJ interactions we use a cutoff r_{cut} around each particle. Inside the cutoff all dipole-dipole interactions are computed explicitly. The electrostatic effects on dipole i due to dipoles beyond r_{cut} are included in the reaction field approximation via the terms $-\frac{1}{2}g\vec{m}_i\cdot\vec{M}_i$ in Eq. (1) and $g\vec{M}_i$, the reaction field, in Eq. (5), where

$$g = \frac{2(\epsilon-1)}{(2\epsilon+1)}\frac{1}{r_{cut}^{3}}, \tag{7}$$

and $\vec{M}_i$ is the total dipole moment inside the cutoff sphere surrounding particle i. ϵ is the static dielectric constant in the system under given conditions computed via

$$\frac{(\epsilon-1)(2\epsilon+1)}{9\epsilon}\vec{E}_i^{ext} = \frac{1}{r_{cut}^{3}}\langle\vec{M}_i\rangle. \tag{8}$$

The details of the above can be found in the Appendix.

Additional quantities derived via the total potential energy are the force and the torque on particle i, i.e.,

$$\vec{F}_i = \vec{F}_{i,LJ} + \sum_{j=1(j\neq i, r_{ij}<r_{cut})}^{N}\left\{\frac{3}{r_{ij}^{5}}[\vec{m}_i(\vec{r}_{ij}\cdot\vec{m}_j) + \vec{m}_j(\vec{r}_{ij}\cdot\vec{m}_i) + \vec{r}_{ij}(\vec{m}_i\cdot\vec{m}_j)] - \frac{15}{r_{ij}^{7}}(\vec{r}_{ij}\cdot\vec{m}_i)(\vec{r}_{ij}\cdot\vec{m}_j)\vec{r}_{ij}\right\}, \tag{9}$$

and

$$\vec{N}_i = \vec{m}_i \times \vec{E}_i = \mu_i \times \vec{E}_i, \tag{10}$$

and the pressure

$$P = P_{LJ} - \frac{1}{2V}\langle\vec{m}_i\mathbf{T}_{ij}\vec{m}_j\rangle + P_{\epsilon}, \tag{11}$$

where P_{ϵ} is given by

TABLE I. ΔT_c at constant $E^{(\infty)}$ or E^{ext}: simulation results and mean field theory.

μ	$E^{(\infty)}$	ΔT_c^{sim}	Ref.	ΔT_c^{MF}
0.5	2.0	0.010	This group	0.010
0.5	6.0	0.069	This group	0.063
0.5	10.0	0.106	This group	0.105
0.5	20.0	0.147	This group	0.159
1.0	0.5	0.005	[11]	0.002
1.0	1.0	0.031	[8]	0.018
1.0	1.0	0.018	[9]	
1.0	1.0	0.017	[11]	
1.0	1.0	0.019	This group	
1.0	1.5	0.034	[9]	0.042
1.0	1.5	0.034	[11]	
1.0	2.0	0.086	[8]	0.069
1.0	2.0	0.053	[9]	
1.0	2.0	0.052	[11]	
1.0	2.0	0.057	This group	
1.0	3.0	0.101	[8]	0.126
1.0	3.0	0.108	This group	
$\sqrt{2}$	0.4	0.004	[9]	0.010
$\sqrt{2}$	0.8	0.038	[9]	0.039
$\sqrt{2}$	1.2	0.073	[9]	0.080
2.0	1.0	0.12	[10]	0.132
2.5	1.0	0.154	[8]	0.128
2.5	2.0	0.265	[8]	0.358
2.5	5.0	0.525	[8]	1.059
μ	E^{ext}	ΔT_c^{sim}	Ref.	ΔT_c^{MF}
0.5	2.0	−0.025	This group	−0.021
0.5	4.0	−0.084	This group	−0.083
1.0	1.0	−0.014	This group	−0.014
1.0	2.0	−0.058	This group	−0.056

$$P_{\epsilon} = -\frac{3\rho}{V}\left\langle\frac{1}{(2\epsilon+1)^2}\left(\vec{m}_i\cdot\vec{A}_i + \frac{\vec{m}_i\cdot\vec{M}_i}{r_{cut}^{3}}\right)\frac{\partial\epsilon}{\partial\rho}\right\rangle \tag{12}$$

with $\vec{A}_i=\vec{E}^{(\infty)}$ if $E^{(\infty)}$ is held constant and $\vec{A}_i=-2\vec{E}^{ext}$ if E^{ext} is held constant instead. We note that potential energy, force, torque, and virial, in the absence of the external field, were worked out by Vesely [23]. We note also that our expression for the reaction field contribution to the pressure differs from the corresponding contribution in Vesely's work because of the neglect of the density dependence of ϵ in the aforementioned reference. Notice in this context that the internal virial may be obtained also via $-3V\partial U/\partial V$. Notice also that the Gibbs ensemble technique used by the other groups listed below in the context of Table I does not require the explicit calculation of the pressure.

The translational motion of the particles is governed by $\ddot{\vec{r}}_i=\vec{F}_i$, whereas the equation of motion governing the dipole

orientation follows via $\vec{N}_i = \mathcal{I}\ddot{\vec{\phi}}_i$. Here $\mathcal{I}$ is the moment of inertia with respect to the momentary axis of rotation. The angle of rotation vector $\vec{\phi}_i$ can be replaced by $\vec{\mu}_i$ using $\dot{\vec{\phi}}_i \times \vec{\mu}_i = \dot{\vec{\mu}}_i$ and $\dot{\vec{\phi}}_i \cdot \vec{\mu}_i = 0$. The resulting equation of motion for $\vec{\mu}_i$ can be found in Sec. 8.2 of Ref. [24] or in the Appendix of Ref. [25]. The equations of motion are integrated using the velocity Verlet algorithm. Temperature, which here is in units of k_B/ϵ (k_B: Boltzmann's constant), is controlled via the weak coupling method of Berendsen *et al.* [26]. Notice that the rotational temperature is given by $(2\mu^2)^{-1}\langle \dot{\vec{\mu}}^2 \rangle = T$. At equilibrium the rotational temperature must be equal to the translational temperature of course. Notice also that here we set the moments of inertia with respect to the major axes equal to one in LJ units. Induced dipole moments may be calculated at every MD step using the iteration scheme $\vec{p}_i^{(k+1)} = \alpha \vec{E}_i(\vec{p}_i^{(k)})$. The dielectric constant is calculated via Eq. (8). G-L phase coexistence curves are obtained by the same method as introduced previously [27,28]; i.e., phase coexistence is established using the Maxwell construction method applied to simulation isotherms at different temperatures. The long-range cutoff, r_{cut}, varies between 4.5 and 5.5.

III. SIMPLE MEAN FIELD DESCRIPTION

A simple mean field description of the g-l transition may be constructed as follows. The orientation partition function, including all dipolar interactions, is given via

$$Q_D \propto \frac{N!}{\Pi_\nu N_\nu!}\left(\frac{\Delta\Omega}{4\pi}\right)^N \exp\left[-T^{-1}\sum_\nu N_\nu u_D(\cos\theta_\nu)\right]. \quad (13)$$

Here the dipoles are sorted in equal size solid angle cones $\Delta\Omega$ whose orientation in space is labeled via the index ν. $u_D(\cos\theta_\nu)$ is given by Eq. (A11) with $\vec{\mu}\cdot\vec{E}_{cav} = \mu E_{cav}\cos\theta$. Application of Stirling's approximation leads to the orientation distribution of the dipoles given via $f(\theta) = \lim_{\Delta\Omega\to 0}(4\pi/\Delta\Omega)N_\nu/N \propto \exp[K\cos\theta]$ with $K = \mu E_{cav}/[(1-\alpha g)T]$. Thus, we obtain for the relevant free energy

$$\frac{\Delta F_D}{NT} = -\ln\left(\frac{\sinh[K]}{K}\right) - \frac{1}{2(1-\alpha g)T}(g\mu^2 + \alpha E_{cav}^2). \quad (14)$$

Notice that it is the first term which accounts for the entropy loss due to orientation in the field. Notice also that in order to evaluate ΔF_D we need ϵ which we compute by solving Eq. (A13) numerically. Our total free energy includes the nondipolar interactions via the van der Waals description, i.e.,

$$\frac{\Delta F_{vdW}}{NT} = \ln\left(\frac{\rho/(3\rho_c^o)}{1-\rho/(3\rho_c^o)}\right) - \frac{9}{8}\frac{\rho/(3\rho_c^o)}{T/(3T_c^o)}. \quad (15)$$

Here ρ_c^o and T_c^o refer to the critical points of the pure LJ system. Thus, $\Delta F = \Delta F_D + \Delta F_{vdW}$ is the free energy contribution governing g-l phase separation.

A similar approach was used by Zhang and Widom to map out the global phase behavior of dipolar fluids [17]. These authors describe the dipolar interactions in terms of the Debye model which differs from the Onsager model used here. In Debye's model the local field includes a term proportional to $\langle\vec{m}\rangle$ instead of the reaction field term proportional to $\vec{m}$ as in Eq. (A7) (for a discussion of this difference see Ref. [29]). We prefer Onsager's approach because of its clearly identifiable approximations. The above-mentioned $\langle\vec{m}\rangle$ proportionality in particular leads to an isotropic liquid-to-ferroelectric liquid transition in the Debye model which is absent in the Onsager model. However, here we are interested in the effect of an electric field on the g-l transition under conditions for which there is no isotropic liquid-to-ferroelectric liquid transition, no association of dipoles into reversible aggregates, usually chains, and no inhomogeneity in the system. The effects of chain formation on the g-l transition were discussed previously in Refs. [27,28]. In general, Onsager's model is a good description of dipolar interaction in simple systems if the parameter $T/(\rho\mu^2)$ is around or larger than unity [29] (assuming $\alpha = 0$).

IV. RESULTS

Figure 1 illustrates the dependence of the static dielectric constant as obtained via mean field theory on the external field strength $\vec{E}^{ext}$. Notice that r_{cut} here refers to Eq. (7). In the mean field approach r_{cut} is the radius of the cavity containing a single dipole. Here $r_{cut} = 0.8$, which we use throughout in all mean field calculations, turns out to yield the overall best agreement between mean field theory and simulation. However, Eq. (7) is used also to estimate the long-range contribution to the electrostatic potential energy. In this case r_{cut} is the radius of the much larger cutoff sphere in the simulation. Figure 2 shows a comparison of the effect of the electric field for the two cases $\vec{E}^{ext} = \text{const}$ and $\vec{E}^{(\infty)} = \text{const}$. Temperature and density are close to the respective critical values for $\mu = 1$ and zero field. Figure 3 compares the density dependence of the static dielectric constant from the simulation to corresponding mean field results.

Figure 4 shows the average dipole-dipole interaction at low densities as obtained by simulation with $\alpha = 0$. We may compare this to the leading contribution to $\langle u_{DD}\rangle$ for weakly correlated dipoles in a weak field

$$\langle u_{DD}\rangle \approx \frac{\rho}{2}4\pi\int_{r>R} dr r^2 \langle u_{DD}\rangle_{orient} \approx -\frac{4\pi\rho}{9}\frac{\mu^4}{TR^3}\left[1 + \frac{1}{1125}\left(\frac{\mu E^{ext}}{T}\right)^4\right], \quad (16)$$

where $\langle u_{DD}\rangle_{orient}$ is the orientational average in the case of weakly correlated dipoles. An analogous calculation carried out for large E^{ext} yields to leading order

$$\langle u_{DD}\rangle \approx -\frac{8\pi\rho}{15}\frac{\mu^4}{TR^3}\left[1 - \left(\frac{T}{\mu E^{ext}}\right)^4\right]. \quad (17)$$

Both limiting laws are included in Fig. 4. For larger densities the above assumptions are no longer valid and the form of $\langle u_{DD}\rangle$ quickly deviates from the above limiting laws. Figure 5 shows simulation results for $\langle u_{DD}\rangle$ for selected conditions, in particular at higher densities, in comparison to corre-

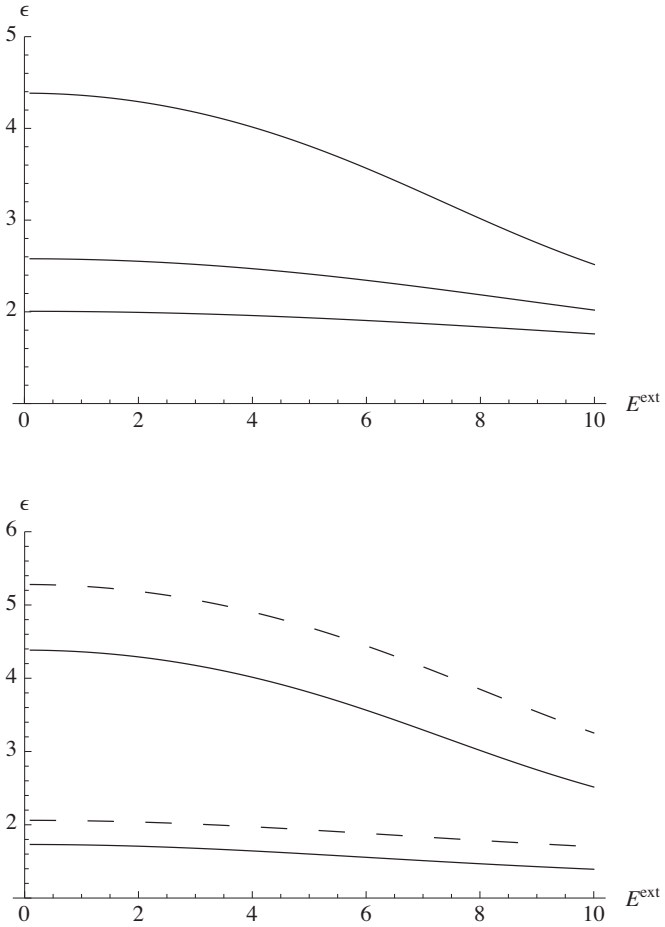

FIG. 1. Mean field dielectric constant ϵ vs the external field E^{ext}. Upper panel: $\rho=0.3$, $\mu=2$, $\alpha=0$, and $T=2,4,6$ (from top to bottom). Lower panel: $\rho=0.3$, $T=2$, $\mu=1$ (lower curve), and $\mu=2$ (upper curve). Corresponding dashed curves with $\alpha=0.05$ ($r_{cut}=0.8$) instead of $\alpha=0$.

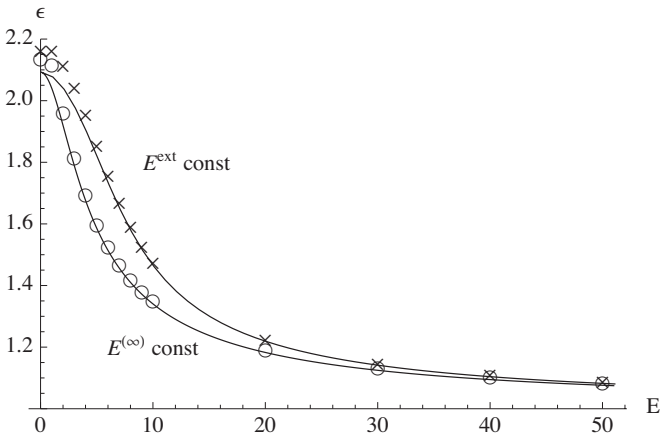

FIG. 2. Static dielectric constant ϵ vs field strength ($\mu=1.0$, $T=1.45$, $\rho=0.3123$). Symbols are simulation results. Crosses: $E=E^{ext}$; circles: $E=E^{(\infty)}$. Note that ϵ at $E=0$ was computed using Eq. (9) in Ref. [29]. The solid lines are computed via mean field theory.

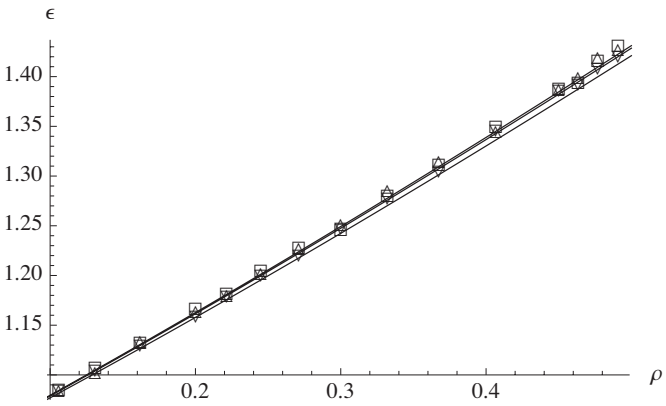

FIG. 3. Static dielectric constant ϵ vs dipole number density ρ ($\mu=0.5$, $T=1.35$). Symbols: simulation results (squares: $E^{ext}=0$; up triangles: $E^{ext}=1$; down triangles: $E^{ext}=2$). Lines (mean field theory) from top to bottom: $E^{ext}=0,1,2$.

sponding curves obtained by computing the first term in Eq. (A11). Qualitatively the Onsager theory agrees with the simulation. Quantitatively we find growing deviation between simulation and the Onsager model as E^{ext} increases.

Figure 6 shows g-l coexistence curves obtained in this work via MD simulation. The values for $\Delta T_c=T_c(\mu,E)-T_c(\mu,0)$, where $E=E^{ext}$ or $E=E^{(\infty)}$, are listed in Table I. The overall comparison between the simulation results and the mean field theory is quite good. In particular we note that the sign of ΔT_c does depend on whether E^{ext} or $E^{(\infty)}$ is held constant. In the latter case the sign is positive whereas in the former it is negative. Figure 6 also reveals a slight shift of the critical density from lower densities for large $E=E^{(\infty)}$ to higher densities at large $E=E^{ext}$. For $\mu=0.5$ this shift certainly is within the scatter of the results, but for $\mu=1.0$ the shift is clearly discernible.

A detailed plot of the reduced mean field critical temperature for $\mu=0.5$ is shown in Fig. 7 (upper panel). We note again that the direction of the critical temperature shift depends on whether the field outside the dielectric is held constant (fixed charge density) or whether the average field in the dielectric is held constant (fixed potential) while density

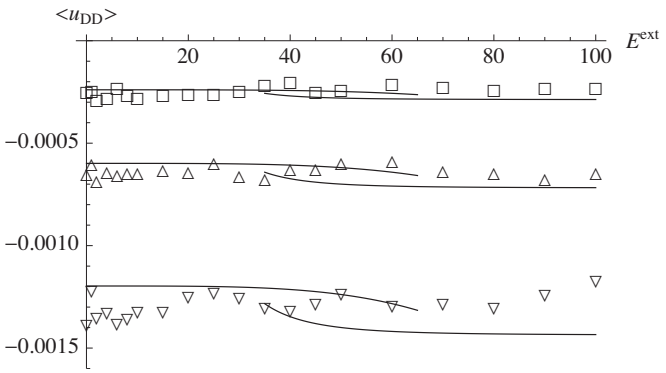

FIG. 4. Average dipole-dipole potential energy $\langle u_{DD}\rangle$ vs $E^{ext}(\mu=0.5, T=10)$. Symbols: simulation results (squares: $\rho=0.02$; up triangles: $\rho=0.05$; down triangles: $\rho=0.1$). Lines: approximations according to Eqs. (16) and (17) with $R=0.9$ plotted to where the correction term exceeds 10% of the leading term.

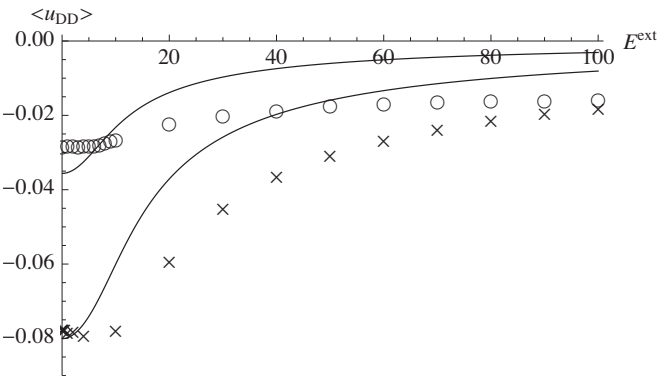

FIG. 5. Average dipole-dipole contribution to the potential energy $\langle u_{DD}\rangle$ vs E^{ext} for $\mu=0.5$ and $\alpha=0$. Open circles: simulation for $\rho=0.308$ at $T=1.351$; crosses: simulation for $\rho=0.8$ at $T=1.332$; lines: corresponding mean field results with $r_{cut}=0.8$ given by the first term in Eq. (A11).

or temperature changes. Notice that we do not include simulation results for $E=E^{ext}$ at large field strength. This is because simulation snapshots at this field strength appear rather inhomogeneous. Figure 7 (bottom panel) also shows a comparison between mean field theory and simulation in the case of the critical density shift, $\Delta\rho_c$, as function of external field strength, E, for $\mu=1.0$. For $E=E^{ext}$ the quantitative agreement is quite good, whereas for $E=E^{(\infty)}$ it is qualitative only.

The sign of ΔT_c depending on the field held constant may be understood as follows. Figure 8 shows the free energy as function of volume (assuming $N=100$ particles) as obtained

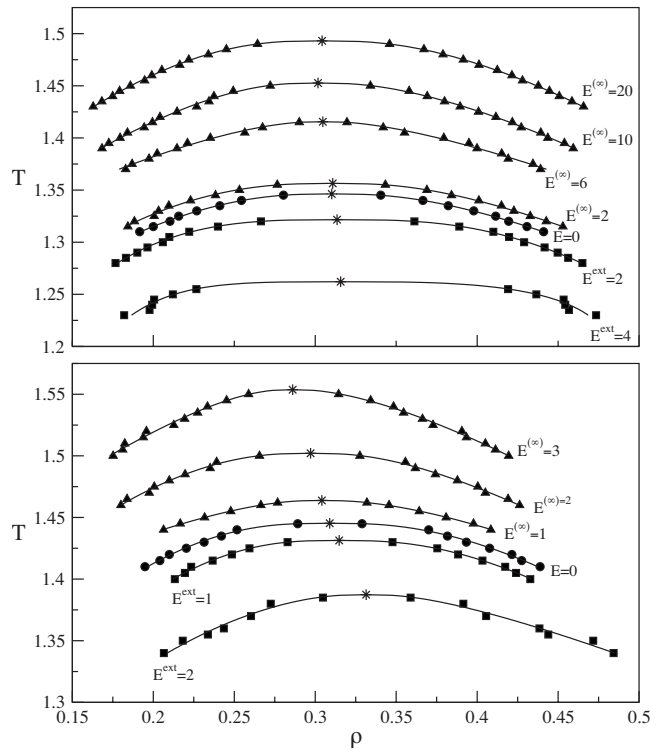

FIG. 6. Coexistence curves in the temperature-number density-plane based on simulation data. Top: $\mu=0.5$; bottom: $\mu=1.0$. In both cases $\alpha=0$. Stars denote critical points. The statistical error is comparable to the size of the symbols.

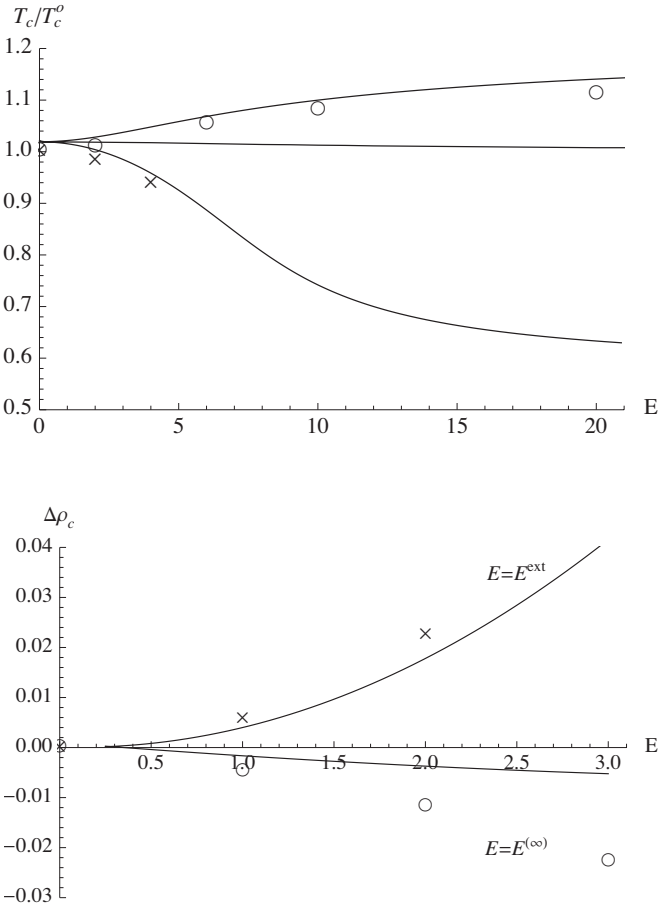

FIG. 7. Top: mean field critical temperature in units of the LJ critical temperature vs E (specified for each curve) for $\mu=0.5$. Symbols are simulation results. Circles: $E=E^{(\infty)}$; crosses: $E=E^{ext}$. Bottom: mean field critical density shift vs E for $\mu=1.0$. Symbols are simulation results. The statistical error again is comparable to the size of the symbols. Circles: $E=E^{(\infty)}$; crosses: $E=E^{ext}$. In all cases $r_{cut}=0.8$, $\rho_c^o=0.3$, $T_c^o=1.32$, and $\alpha=0$.

via mean field theory. The solid (dashed) line corresponds to $E^{(\infty)}$ (E^{ext}) held constant. The dotted line is the zero field result. The temperature is below the critical temperature and we observe a van der Waals loop. The two lower panels in Fig. 8 show the attendant comparison for the orientation contribution to the free energy according to the first term in Eq. (14), f_{orient}, and the contribution due to dipolar interaction described by the second term in Eq. (14), f_{DD}. We notice that the latter virtually remains unaltered whereas f_{orient} accounts for the difference. Due to $\vec{E}^{ext}=\epsilon\vec{E}^{(\infty)}$ we find that constant E^{ext} implies a reduction in $E^{(\infty)}$ when the density is increased because ϵ increases. Notice also that at this small field strength ϵ is basically independent of field strength. Because of relation (A15) between $\vec{E}^{(\infty)}$ and $\vec{E}_{cav}$, which governs orientation in the field, the quantity K in Eq. (14), and therefore the orientation, is reduced when $E^{(\infty)}$ is reduced. This means that for constant E^{ext} the free energy contribution f_{orient} increases with increasing density, which in turn diminishes the van der Waals loop in comparison to the zero field case; i.e., ΔT_c is negative. The reverse is true when $\vec{E}^{(\infty)}$ is held constant. Here f_{orient} decreases with increasing density, which in

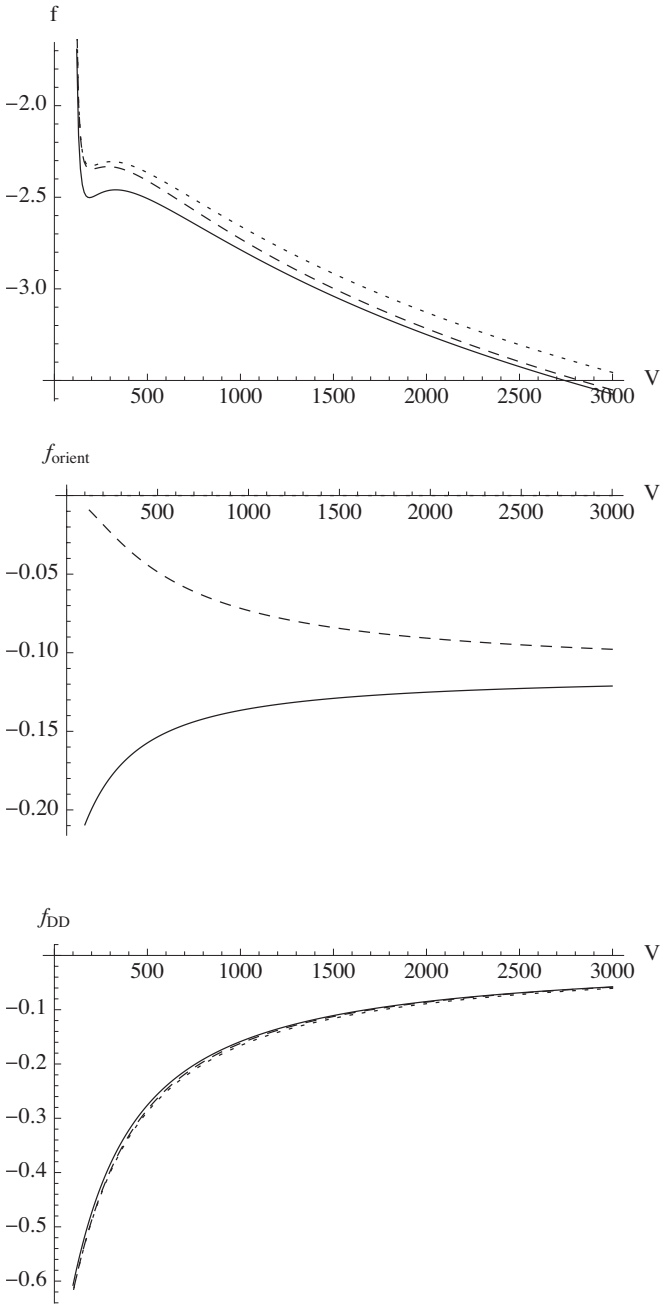

FIG. 8. Top: $f=\Delta F/(NT)$ vs volume V; middle: f_{orient}, according to the first term in Eq. (14), vs V; bottom: f_{DD}, according to the second term in Eq. (14), vs V. In all cases $\mu=1.0$, $T=1.2$, $r_{cut}=0.8$, $\rho_c^o=0.3$, $T_c^o=1.32$, and $\alpha=0$. Solid lines: $E^{(\infty)}=1$ is held constant; dashed lines: $E^{ext}=1$ is held constant; dotted lines: zero field.

turn enhances the van der Waals loop in comparison to the zero field case; i.e., ΔT_c is positive. Figure 9 shows this effect in terms of the average projection of $\vec{\mu}/\mu$ onto the direction of the electric field for $\mu=0.5, 1.0$ and $T=1.2$. We note that the agreement between the mean field theory and the simulation is quite reasonable. We also note that in general the scatter of the simulation results is larger for $\vec{E}^{ext}$ held constant than for $\vec{E}^{(\infty)}$ held constant. In both cases each point is based on 1.5×10^6 MD steps (of which 10^6 were used for averaging) and a step width of 3×10^{-3}.

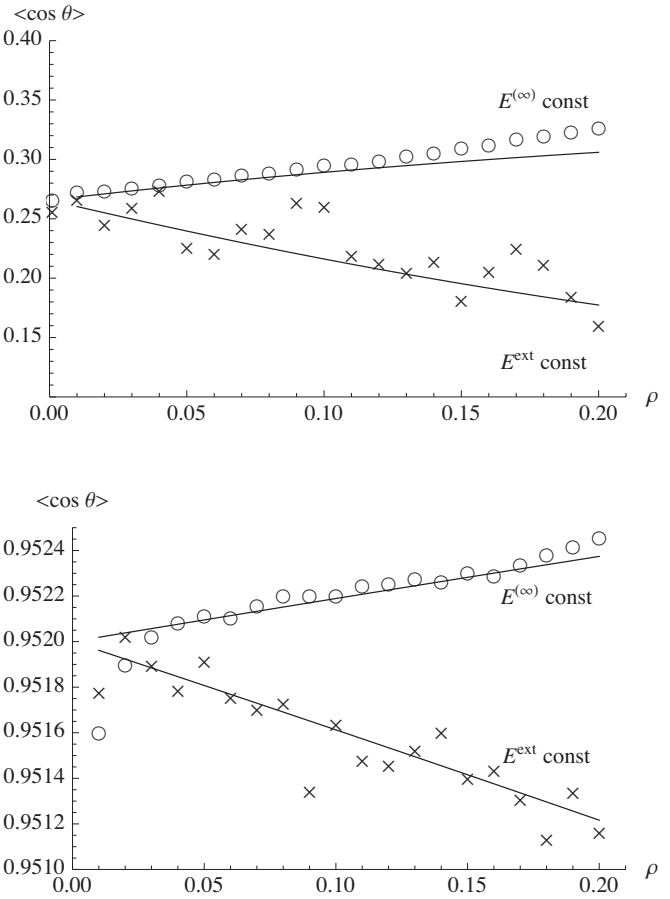

FIG. 9. Top: Average orientation of the dipoles relative to the electric field direction, $\langle\cos\theta\rangle$, vs density, ρ, for $\mu=1$ and $T=1.2$. Solid lines: mean field theory; open circles: simulation result for $E^{(\infty)}=1$; crosses: simulation result for $E^{ext}=1$. Bottom: same as above but for $\mu=0.5$, $E^{(\infty)}=50$, and $E^{ext}=50$.

It is interesting to compare the electric field dependence of the critical temperature discussed above with the textbook expression in Ref. [14], which is given by

$$\Delta T_c \approx \frac{1}{8\pi}\rho_{c,E=0}E^2\frac{(\partial^2\epsilon/\partial\rho^2)_{T=T_{c,E=0},E}}{(\partial^2 P/\partial\rho\,\partial T)_{T_{c,E=0},E=0}}. \tag{18}$$

Provided that ΔT_c is small this result is rather general. The field E in this case is $E^{(\infty)}$. In order to compare with the result in Fig. 7 we compute the denominator via van der Waals theory, i.e., $(\partial^2 P/\partial\rho\partial T)_{T_{c,E=0},E=0}=9/4$ (this number is roughly half what one obtains based on the actual simulation data). The derivative in the numerator is computed using Onsager's expression for ϵ in Eq. (A14) (with $\alpha=0$). The result is the dashed line in Fig. 10 shown together with the previous mean field result for constant $\vec{E}^{(\infty)}$ taken from Fig. 7. The deviation on the high field side occurs because in the Onsager theory ϵ itself depends on E. This is explicitly excluded in the derivation of Eq. (18).

Computer simulations of dipolar fluids in an external field $\vec{E}_o$ usually are based on the following general approach. The field couples to the system via $-\Sigma_i\vec{\mu}_i\cdot\vec{E}_o$ in the Hamiltonian [cf. Eq. (1)]. The sum extends over all dipole moments

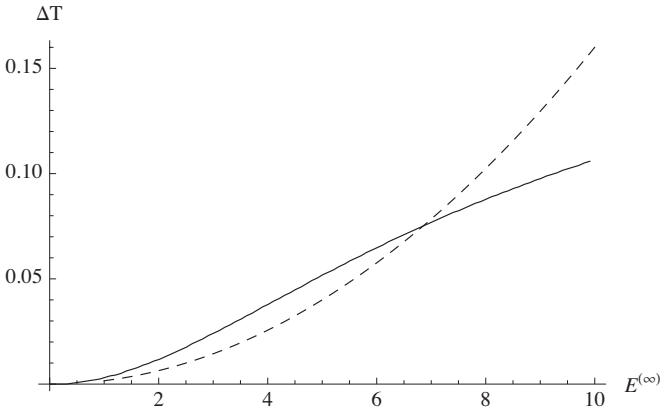

FIG. 10. Critical temperature shift ΔT_c vs $E^{(\infty)}$ for $\mu=0.5$. Solid line: mean field theory developed in this work; dashed line: ΔT_c as derived in Ref. [14].

$\vec{\mu}_i$. Ewald summation is used in conjunction with a continuum (dielectric constant ϵ_{out}) surrounding the sphere of explicit summation. The average field in the liquid (Maxwell field), $\vec{E}$, and $\vec{E}_o$ are related via $\vec{E}=\vec{E}_o-4\pi\vec{P}/(2\epsilon_{out}+1)$ (see [30]). The polarization of the liquid of dipolar particles is tied to the Maxwell field via $4\pi\vec{P}=(\epsilon_{in}-1)\vec{E}$, where ϵ_{in} is the dielectric constant of this liquid and thus $\vec{E}_o=(2\epsilon_{out}+\epsilon_{in})/(2\epsilon_{out}+1)\vec{E}$. In the literature discussed in the following paragraph this is the method of choice.

The following is, to the best of our knowledge, a complete list of simulation studies addressing the critical point shift in a pure dipolar liquid. Stevens and Grest [8] have used Gibbs ensemble Monte Carlo simulations of the Stockmayer fluid in an applied field. They use tin-foil boundary conditions, which according to the preceding paragraph means $\vec{E}_o=\vec{E}=\vec{E}^{(\infty)}$. In Ref. [9] the authors study the influence of static electric fields on the vapor-liquid coexistence of dipolar soft-sphere and Stockmayer fluids both via Gubbins-Pople-Stell perturbation theory and simulation. Again the applied field corresponds to $E^{(\infty)}$ because the simulations were performed in the reaction field geometry with conducting boundary conditions, where the spherical sample is embedded in a continuum with infinite dielectric constant. In Ref. [10] the authors carry out Gibbs ensemble simulations of the Stockmayer fluid in an applied field $\vec{E}_o$. The authors compare the cases $\epsilon_{out}=\infty$ (tin-foil), i.e., $\vec{E}_o=\vec{E}$, $\epsilon_{out}=\epsilon_{in}$, i.e., $\vec{E}_o=3\epsilon_{in}(2\epsilon_{in}+1)^{-1}\vec{E}$, and $\epsilon_{out}=1$ (vacuum), i.e., $\vec{E}_o=(\epsilon_{in}+2)/3\vec{E}$. Even though the authors do not compute T_c explicitly it is still possible to compare the relative order of T_c for the three boundary conditions based on their Fig. 2; i.e., T_c decreases in the order of discussion. Moreover $T_c(\epsilon_{out}=\infty)$ is certainly above the T_c in absence of a field, whereas $T_c(\epsilon_{out}=\epsilon_{in})$ is close to T_c in absence of a field. This is consistent with our Fig. 7, where the curves labeled $E=E^{(\infty)}$ and $E=E^{cav}$ correspond to these two cases. $T_c(\epsilon_{out}=1)$ appears to be below the zero field critical temperature. This we expect according to our discussion of Fig. 7 because E is decreased with increasing density. In Ref. [11] the authors study hard-core dipolar Yukawa fluids using the *NPT*-Monte Carlo plus test particle method in conjunction with reaction field long-range corrections and conducting boundaries for the dipole-dipole interactions. Their results for ΔT_c correspond to $\vec{E}_o=\vec{E}=\vec{E}^{(\infty)}$. In Table I we list the simulation results for the shift of the critical temperature, ΔT_c^{sim}, for various dipole moments and field strengths extracted from these references, supplemented by our own results, which all use the Stockmayer potential (with the exception of Ref. [11]). In addition we compute the corresponding ΔT_c^{MF} from our simple mean field theory, which overall is in fair agreement with the literature simulation data. Notice that ΔT_c is small compared to T_c and that the errors involved in the determination of T_c are often enough comparable to ΔT_c.

The number of theoretical studies of g-l coexistence in dipolar fluids under influence of an external electric field is far more numerous. To our knowledge the first work dealing with this problem in detail, aside from the above textbook formula, is Ref. [16]. Using density-functional theory the authors consider a sample of fluid in the field constrained to have a spherical shape—apparently surrounded by vacuum. They find a negative ΔT upon increasing E_o in agreement with our above discussion and the $\epsilon_{out}=1$ result in Ref. [10]. Other studies [19], (Gubbins-Pople-Stell perturbation theory) [20], (density-functional theory) [21], (modified mean field density-functional theory) [22], (self-consistent theory based on mean spherical approximation for the dipolar Yukawa fluid), are more complicated, with the exception of Ref. [17] already mentioned and usually less transparent but do not yield obvious improvements over the simple theory used here. The other simple theory, i.e., Ref. [17], which is based on the Debye model, seems to perform less well than the one used here, which is based on Onsager's refinement.

V. CONCLUSION

Using the MD technique we have computed g-l phase coexistence curves for the Stockmayer fluid in an external field. We observe a field-induced shift of the critical temperature ΔT_c. Whether the critical temperature is increased or decreased depends on whether potential or surface charge density are kept constant assuming that the dielectric material fills the space between capacitor plates. Our own as well as previous literature data for ΔT_c are compared to and interpreted in terms of a simple mean field theory. Despite considerable errors in the simulation results, we find that there is consistency between the simulation results obtained by different groups and the mean field description. The latter ties the sign of ΔT_c to the outside constraints via the electric field dependence of the orientation part of the mean field free energy.

APPENDIX

The terms in Eq. (1) describing explicit interactions between point dipole moments as well as their interaction with the external field, U_{DD}, may be cast in various equivalent forms. The probably most transparent one is

$$U_{DD} = -\frac{1}{2}\vec{\mu}_i \mathbf{T}_{ij}\vec{\mu}_j - \vec{\mu}_i \cdot \vec{E}_i^{ext} - \frac{1}{2}\vec{p}_i \cdot \vec{E}_i^{(o)}. \quad \text{(A1)}$$

Here the first and second terms describe the interaction of permanent dipoles with each other and with an external field. The last term describes the total decrease in energy if a polarizable medium is brought in an electrical field with fixed sources (e.g., Sec. 4.7 in Ref. [31]), i.e., the permanent dipole moments at fixed orientation plus the external field due to likewise fixed sources. Here

$$\vec{E}_i^{(o)} = \mathbf{T}_{ij}\vec{\mu}_j + \vec{E}_i^{ext}. \quad \text{(A2)}$$

Equation (A1) may be rewritten as

$$U_{DD} = -\frac{1}{2}\vec{m}_i \cdot \vec{E}_i^{(o)} - \frac{1}{2}\vec{\mu}_i \cdot \vec{E}_i^{ext} \quad \text{(A3)}$$

or

$$U_{DD} = -\frac{1}{2}\vec{\mu}_i \cdot \vec{E}_i - \frac{1}{2}\vec{m}_i \cdot \vec{E}_i^{ext}, \quad \text{(A4)}$$

where $\vec{E}_i$ is given by Eq. (5) omitting the last term, or

$$U_{DD} = -\frac{1}{2}\vec{m}_i \mathbf{T}_{ij}\vec{m}_j + \frac{1}{2}\frac{\vec{p}_i^2}{\alpha} - \vec{m}_i \cdot \vec{E}_i^{ext} \quad \text{(A5)}$$

[cf. Eq. (1)], making use of Eq. (4) of course.

In the context of computer simulation of dielectric constants in soft condensed-matter systems U_{DD} usually appears as

$$U_{DD} = -\frac{1}{2}\vec{\mu}_i \mathbf{T}_{ij}\vec{m}_{o,j} - \vec{m}_{o,i} \cdot \vec{E}_i^{ext} - \frac{1}{2}\vec{E}_i^{ext}(\mathbf{A}_{ij}\vec{E}_j^{ext}), \quad \text{(A6)}$$

where $\vec{m}_{o,j} = (\delta_{ij} - \alpha \mathbf{T}_{ij})^{-1}\vec{\mu}_i$ and $\mathbf{A}_{ij} = \alpha(\delta_{ij} - \alpha \mathbf{T}_{ij})^{-1}$. Note that here $\vec{m}_i = \vec{\mu}_i + \alpha(\mathbf{T}_{ij}\vec{m}_j + \vec{E}_i^{ext})$ is solved for $\vec{m}_j = \vec{m}_{o,j} + \mathbf{A}_{ij}\vec{E}_i^{ext}$ [32,33].

Thus far the meaning of the external field, $\vec{E}_i^{ext}$, is clear. It is the external field felt at the position of dipole i in the system. The need for specific boundary conditions, however, makes it necessary to precisely specify the relation of $\vec{E}_i^{ext}$ to the average field inside the dielectric material $\vec{E}^{(\infty)}$ or to the external field outside the dielectric material, $\vec{E}^{ext}$. This is particularly relevant for the comparison to experiments or other simulation results.

In the present case, the reaction field approach to long-range interaction, we assume that every dipole moment interacts explicitly with all other dipole moments within a spherical shell of radius r_{cut}. Beyond r_{cut} there is a dielectric continuum characterized by a dielectric constant ϵ. A simplified version of this situation has been studied by Onsager in his famous paper on the electric moments of molecules in liquids [34]. It is instructive to compare key expressions of this continuum approach to the analogous expressions used in the simulation. Onsager considers a single dipole moment $\vec{m}$ akin to $\vec{m}_i$ in Eq. (3). The dipole moment $\vec{m}$ feels an electric field

$$\vec{E}_{in} = g\vec{m} + \vec{E}_{cav}. \quad \text{(A7)}$$

The first term is the reaction field. Notice that in this case r_{cut} in Eq. (7) is the radius of the cavity occupied by the dipole $\vec{m}$ only. $\vec{E}_{cav}$, the second term, is the so-called cavity field given by

$$\vec{E}_{cav} = \frac{3\epsilon}{2\epsilon + 1}\vec{E}^{(\infty)}, \quad \text{(A8)}$$

where ϵ is the dielectric constant of the surrounding medium and $\vec{E}^{(\infty)}$ is a homogeneous electric field at large distances from the cavity due to external sources. The calculation of $\vec{E}_{in}$ on the basis of Maxwell's equations in dielectric media can be found in Appendix A.2 of Fröhlich's book on the theory of dielectrics [35] as well as in the original paper of course. In analogy to Eq. (A3) the potential energy of the dipole at the center of the cavity is

$$u_D = -\frac{1}{2}\vec{m} \cdot (g\vec{\mu} + \vec{E}_{cav}) - \frac{1}{2}\vec{\mu} \cdot \vec{E}_{cav}. \quad \text{(A9)}$$

Using $\vec{p} = \alpha\vec{E}_{in}$, i.e., Eq. (4), we may rewrite this into

$$u_D = -\frac{1}{2}\vec{m} \cdot g \cdot \vec{m} + \frac{1}{2}\frac{\vec{p}^2}{\alpha} - \vec{m} \cdot \vec{E}_{cav}. \quad \text{(A10)}$$

This result corresponds to Eq. (A5). Rewriting $\vec{m}$ as $\vec{m} = (1 - \alpha g)^{-1}\vec{\mu} + \alpha(1 - \alpha g)^{-1}\vec{E}_{cav}$ yields yet another expression, i.e.,

$$u_D = -\frac{1}{2}\frac{g}{1 - \alpha g}\mu^2 - \frac{1}{1 - \alpha g}\vec{\mu} \cdot \vec{E}_{cav} - \frac{1}{2}\frac{\alpha}{1 - \alpha g}\vec{E}_{cav}^2. \quad \text{(A11)}$$

This is the analog of Eq. (A6), which generalizes Onsager's calculation to more than one dipole inside the cavity [32,36].

It is worth noting that this form of u_D is particular suitable to compute $\langle \vec{m} \rangle$ because we merely need to compute $\langle \vec{\mu} \rangle$ using the Boltzmann weight $\exp[(1 - \alpha g)^{-1}\vec{\mu} \cdot \vec{E}_{cav}/T]$. The result is

$$\langle \vec{m} \rangle = \mathcal{L}(x)\frac{\mu}{1 - \alpha g}\vec{e}_z + \frac{\alpha}{1 - \alpha g}\vec{E}_{cav}, \quad \text{(A12)}$$

with $\mathcal{L}(x) = \coth(x) - x^{-1}$ and $x = (1 - \alpha g)^{-1}\mu E_{cav}/T$. Here $\vec{e}_z$ is a unit vector parallel to the cavity field. Using the relation $\rho\langle \vec{m} \rangle = \vec{P} = (\epsilon - 1)\vec{E}^{(\infty)}/(4\pi)$, where $\vec{P}$ is the polarization, together with Eq. (A8) we obtain the result

$$\frac{1}{4\pi\rho}\frac{(\epsilon - 1)(2\epsilon + 1)}{3\epsilon}\vec{E}_{cav} = \mathcal{L}(x)\frac{\mu}{1 - \alpha g}\vec{e}_z + \frac{\alpha}{1 - \alpha g}\vec{E}_{cav}, \quad \text{(A13)}$$

and in the limit $E^{(\infty)} \to 0$,

$$\frac{1}{4\pi\rho}\frac{(\epsilon - 1)(2\epsilon + 1)}{3\epsilon} = \frac{1}{3T}\left(\frac{\mu}{1 - \alpha g}\right)^2 + \frac{\alpha}{1 - \alpha g}. \quad \text{(A14)}$$

This formula obtained by Onsager relates the microscopic dipole moment, μ, and polarizability, α, to the macroscopic

dielectric constant ϵ [34]. Its interesting relation to Debye's earlier equation [37] is discussed in Ref. [29].

If we now consider a spherical cavity occupied by a number of dipole moments $\vec{m}_i$ we may directly obtain the reaction field corrections to U in Eq. (1) and $\vec{E}_i$ in Eq. (5). Notice that the reaction field now becomes $g\vec{M}_i$, where $M_i = \Sigma_{j \in V_{cav}} \vec{m}_j$ (including $\vec{m}_i$). Thus, comparing Eq. (A5) to Eq. (A10) leads to Eq. (1) and comparing the first two terms in Eq. (5) to Eq. (A7) leads to the full Eq. (5).

In particular we also note that $\vec{E}_i^{ext}$ corresponds to $\vec{E}_{cav}$. Via Eq. (A8) we may therefore relate $\vec{E}_i^{ext}$ to $\vec{E}^{(\infty)}$. We now consider a (small) cavity embedded in a homogenous slab of dielectric material (like in the case of an infinite plate capacitor filled with dielectric material). Assuming a constant field $\vec{E}^{ext}$ outside the dielectric and perpendicular to the adjacent slab surfaces we have $\vec{E}^{ext} = \epsilon \vec{E}^{(\infty)}$. Thus, we find

$$\vec{E}_i^{ext} = \frac{3}{2\epsilon + 1} \vec{E}^{ext}. \tag{A15}$$

Unless stated otherwise we will use this relation throughout. Notice in particular that Eq. (8) follows via $\langle \vec{M}_i \rangle / (4\pi r_{cut}^3/3) = (\epsilon - 1)\vec{E}^{(\infty)}/(4\pi)$ in conjunction with Eq. (A15).

[1] C. Holm and J.-J. Weis, Curr. Opin. Colloid Interface Sci. **10**, 133 (2005).
[2] J.-J. Weis and D. Levesque, in *Advanced Computer Simulation Approaches for Soft Matter Sciences II*, Advances in Polymer Science Vol. 185, edited by C. Holm and K. Kremer (Springer, New York, 2005).
[3] S. H. L. Klapp, J. Phys.: Condens. Matter **17**, R525 (2005).
[4] B. Huke and M. Lücke, Rep. Prog. Phys. **67**, 1731 (2004).
[5] M. A. Pounds and P. A. Madden, J. Chem. Phys. **126**, 104506 (2007).
[6] D. P. Shelton and Z. Quine, J. Chem. Phys. **127**, 204503 (2007), and references therein.
[7] G. Ganzenmüller, G. N. Patey, and P. J. Camp, Mol. Phys. **107**, 403 (2009).
[8] M. J. Stevens and G. S. Grest, Phys. Rev. E **51**, 5976 (1995).
[9] D. Boda, J. Winkelmann, J. Liszi, and I. Szalai, Mol. Phys. **87**, 601 (1996).
[10] K. Kiyohara, K. J. Oh, X. C. Zeng, and K. Ohta, Mol. Simul. **23**, 95 (1999).
[11] I. Szalai and S. Dietrich, J. Phys.: Condens. Matter **20**, 204122 (2008).
[12] We note that Lado *et al.* [38] have determined phase coexistence curves for a classical Heisenberg spin fluid with short-range interactions in an external magnetic field. They observe an increase in the critical temperature with increasing field strength.
[13] P. Debye and K. Kleboth, J. Chem. Phys. **42**, 3155 (1965).
[14] L. D. Landau and E. M. Lifschitz, *Electrodynamics of Continuous Media* (Pergamon Press, New York, 1984), Vol. 8.
[15] J. R. Quint, J. A. Gates, and R. H. Wood, J. Phys. Chem. **89**, 2647 (1985).
[16] C. E. Woodward and S. Nordholm, J. Phys. Chem. **92**, 501 (1988).
[17] H. Zhang and M. Widom, Phys. Rev. E **49**, R3591 (1994).
[18] A. Onuki, Europhys. Lett. **29**, 611 (1995).
[19] D. Boda, I. Szalai, and J. Liszi, J. Chem. Soc., Faraday Trans. **91**, 889 (1995).
[20] B. Groh and S. Dietrich, Phys. Rev. E **53**, 2509 (1996).
[21] V. B. Warshavsky and X. C. Zeng, Phys. Rev. E **68**, 051203 (2003).
[22] I. Szalai, K.-Y. Chan, and Y. W. Tang, Mol. Phys. **101**, 1819 (2003).
[23] F. J. Vesely, J. Comput. Phys. **24**, 361 (1977).
[24] D. C. Rapaport, *The Art of Molecular Dynamics Simulation* (Cambridge University Press, Cambridge, 1995).
[25] W.-Z. Ouyang and R. Hentschke, J. Chem. Phys. **127**, 164501 (2007).
[26] H. J. C. Berendsen, J. P. M. Postma, W. F. van Gunsteren, A. DiNola, and J. R. Haak, J. Chem. Phys. **81**, 3684 (1984).
[27] R. Hentschke, J. Bartke, and F. Pesth, Phys. Rev. E **75**, 011506 (2007).
[28] J. Bartke and R. Hentschke, Phys. Rev. E **75**, 061503 (2007).
[29] J. Bartke and R. Hentschke, Mol. Phys. **104**, 3057 (2006).
[30] This formula is derived in Appendix A.2 of Ref. [35]. Note, however, that the dielectric constant ϵ_2 in A.2 is unity in the present case because it refers to an "extra" underlying continuum and should not be confused with ϵ_{in}.
[31] J. D. Jackson, *Classical Electrodynamics* (John Wiley & Sons, New York, 1975).
[32] M. Mandel and P. Mazur, Physica **24**, 116 (1958).
[33] E. L. Pollock, B. J. Alder, and G. N. Patey, Physica A **108**, 14 (1981).
[34] L. Onsager, J. Am. Chem. Soc. **58**, 1486 (1936).
[35] H. Fröhlich, *Theory of Dielectrics* (Oxford University Press, London, 1958).
[36] J. G. Kirkwood, J. Chem. Phys. **7**, 911 (1939).
[37] P. Debye, *Polare Molekeln* (Hirzel Verlag, Leipzig, 1929).
[38] F. Lado, E. Lomba, and J. J. Weis, Phys. Rev. E **58**, 3478 (1998).